1 **Coding and regulatory variants affect serum protein levels and common disease**

5 Valur Emilsson[1,2,ξ,*], Valborg Gudmundsdottir[1,ξ], Alexander Gudjonsson[1,ξ], Mohd A
6 Karim[3,4], Marjan Ilkov[1], James R. Staley[5], Elias F. Gudmundsson[1], Brynjolfur G. Jonsson[1],
7 Lenore J. Launer[6], Jan H. Lindeman[7], Nicholas M. Morton[8], Thor Aspelund[1], John R. Lamb[9],
8 Lori L. Jennings[10] and Vilmundur Gudnason[1,2,*]

12 [1]Icelandic Heart Association, Holtasmari 1, IS-201 Kopavogur, Iceland.
13 [2]Faculty of Medicine, University of Iceland, 101 Reykjavik, Iceland
14 [3]Wellcome Trust Sanger Institute, Welcome Genome Campus, Hinxton, Cambridgeshire
15 CB10 1SA, UK.
16 [4]Open Targets, Wellcome Genome Campus, Hinxton, Cambridgeshire CB10 1SD, UK
17 [5]MRC/BHF Cardiovascular Epidemiology Unit, Department of Public Health and Primary
18 Care, University of Cambridge, Cambridge, UK
19 [6]Laboratory of Epidemiology and Population Sciences, Intramural Research Program,
20 National Institute on Aging, Bethesda, MD 20892-9205, USA.
21 [7]Department of General Surgery Leiden University Medical Center, Leiden. Holland
22 [8]Centre for Cardiovascular Sciences, Queen's Medical Research Institute, University of
23 Edinburgh, Edinburgh EH16 4TJ, UK
24 [9]GNF Novartis, 10675 John Jay Hopkins Drive, San Diego, CA 92121, USA.
25 [10]Novartis Institutes for Biomedical Research, 22 Windsor Street, Cambridge, MA 02139,
26 USA.

34 [ξ]These authors contributed equally.
35 [*]Corresponding authors. Emails: valur@hjarta.is and v.gudnason@hjarta.is

Abstract

Circulating proteins are prognostic for human outcomes including cancer, heart failure, brain trauma and brain amyloid plaque burden. A deep serum proteome survey recently revealed close associations of serum protein networks and common diseases. The present study reveals unprecedented number of individual serum proteins that overlap genetic signatures of diseases emanating from different tissues of the body. Here, 54,469 low-frequency and common exome-array variants were compared with 4782 protein measurements in the serum of 5343 individuals of the deeply annotated AGES Reykjavik cohort. Using a study-wide significant threshold, 2019 independent exome array variants affecting levels of 2135 serum proteins were identified. These variants overlapped genetic loci for hundreds of complex disease traits, emphasizing the emerging role for serum proteins as biomarkers of and potential causative agents of multiple diseases.

Large-scale genome-wide association studies (GWASs) have expanded our knowledge of the genetic basis of complex disease. As of 2018, approximately 5687 GWASs have been published revealing 71,673 DNA variants to phenotype associations[1]. Furthermore, exome-wide genotyping arrays have linked rare and common variants to many complex traits. For example, 444 independent risk variants were recently identified for lipoprotein fractions across 250 genes[2]. Despite the overall success of GWAS, the common lead SNPs rarely point directly to a clear causative polymorphism, making determination of the underlying disease mechanism difficult[3-6]. Regulatory variants affecting mRNA and/or protein levels and structural variants like missense mutations can point directly to the causal candidate. Alteration of the amino acid sequence may affect protein activity and/or influence transcription, translation, stability, processing, and secretion of the protein in question[7-9].

61   Thus, by integrating intermediate traits like mRNA and/or protein levels with genetics and

62   disease traits, the identification of the causal candidates can be enhanced[3-6].

63   Proteins are arguably the ultimate players in all life processes in disease and health, however,

64   high throughput detection and quantification of proteins has been hampered by the limitations

65   of available proteomic technologies. Recently, a custom-designed Slow-Off rate Modified

66   Aptamer (SOMAmer) protein profiling platform was developed to measure 4782 proteins

67   encoded by 4137 human genes in the serum of 5457 individuals from the AGES Reykjavik

68   study (AGES-RS)[10], resulting in 26.1 million individual protein measurements. Various

69   metrics related to the performance of the proteomic platform including aptamer specificity,

70   assay variability and reproducibility have already been described[10]. We demonstrated that the

71   human serum proteome is under strong genetic control[10], in line with findings of others

72   applying identical or different proteomics technologies[11,12]. Moreover, serum proteins were

73   found to exist in regulatory groups of network modules composed of members synthesized in

74   all tissues of the body, suggesting that system level coordination or homeostasis is mediated

75   to a significant degree by thousands of proteins in blood[13]. Importantly, the deep serum and

76   plasma proteome is associated with and prognostic for various diseases as well as human life

77   span[10,14-20].

78   Here, we regressed levels of 4782 proteins on 54,469 low-frequency and common variants

79   from the HumanExome BeadChip exome array, in sera from 5343 individuals of the deeply

80   phenotyped AGES-RS cohort. Further cross-referencing of all significant genotype-to-protein

81   associations to hundreds of genetic loci for various disease endpoints and clinical traits,

82   demonstrated profound overlap between the genetics of circulating proteins and disease

83   related phenotypes. We highlight how triangulation of data from different sources can link

84   genetics, protein levels and disease(s), with the intention of cross-validating one another and

85   point to potentially causal relationship between proteins and complex disease(s).

86   Using genotype data from an exome array (HumanExome BeadChip) enriched for structural

87   variants and tagged for many GWAS risk loci (**Methods**), the effect of low-frequency and

88   common variants on the deep serum proteome was examined. Quality control filters[21], and

89   exclusion of monomorphic variants reduced the available variants to 76,891. Additionally, we

90   excluded variants at minor allele frequency (MAF) < 0.001 as they provide insufficient power

91   for single-point association analysis[22]. This resulted in 54,469 low-frequency (54%,

92   MAF<0.05) and common variants (46%, MAF ≥0.05) that were tested for association to each

93   of the 4782 human serum protein measurements using linear regression analysis adjusted for

94   the confounders age and sex (**Methods**). The current platform targets the serum proteome

95   arising largely from active or passive secretion, ectodomain shedding, lysis and/or cell

96   death[10,23]. **Figure 1a** highlights the classification of the protein population targeted by the

97   aptamer-based profiling platform, showing over 68.7% of the proteins are secreted or single

98   pass transmembrane (SPTM) receptors.

99   Applying a Bonferroni corrected significance threshold of $P < 1.92 \times 10^{-10}$ (0.05/54469/4782)

100   we detected 5472 exome array variants that were associated with variable levels of 2135

101   serum proteins (**Supplementary Table 1** and **Fig. 1b**), of which 2019 variants are

102   independent (**Supplementary Table S2**). **Supplementary Table 1** lists all associations at P-

103   value $< 1 \times 10^{-6}$, or 10,200 exome array variants affecting 3096 human proteins. These protein

104   quantitative trait loci (pQTLs) were *cis* and/or *trans* acting including several *trans* acting

105   hotspots with pleiotropic effects on multiple co-regulated proteins (**Fig. 1b**). Secreted proteins

106   were enriched for pQTLs (P-value < 0.0001) as compared to non-secreted proteins using

107   10,000 permutations to obtain the empirical distribution of the χ^2 test of equality of

108   proportions (**Supplementary Fig. S1**). This suggests that proteins bound for the systemic

109   environment are subject to more genetic regulation than other proteins identified by the

110   current platform. **Supplementary Table S3** summarizes various pathogenicity prediction

111   scores for all independent study-wide significant pQTLs in **Supplementary Table S2**, using

112   the Ensembl Variant Effect Predictor (VEP)[24,25]. Next, we cross-referenced all the 5472

113   study-wide significant pQTLs with a comprehensive collection of genetic loci associated with

114   diseases and clinical traits from the curated PhenoScanner database[26], revealing that 60% of

115   all pQTLs were linked to at least one disease-related trait (**Supplementary Table S4**). We

116   have shown in our previous studies that genetic loci affecting several serum proteins exhibit

117   pleiotropy in relation to complex diseases[10]. An example of a possible pleiotropic effect

118   mediated by the variant rs2251219 within the gene *PBRM1* affecting multiple proteins and

119   sharing genetics with various diseases and clinical features is illustrated in **Fig. 2**.

120   **Supplementary Fig. S2** depicts the relationship between all proteins and some quantitative

121   traits associated with rs2251219. **Table 1** highlights a selected set of pQTLs that share

122   genetics with diseases of different etiologies including disorders of the brain, metabolism,

123   immune and cardiovascular system and cancer. In the sections that follow, we give examples

124   of serum pQTLs that overlap disease risk loci and demonstrate how different data sources can

125   cross-validate one another. Although data triangulation can be used to infer directional

126   consistency, it cannot tell whether the relationship is causal or reactive to a given outcome. As

127   a result, we used two-sample Mendelian randomization analysis (MR) on highlighted

128   examples to test support for a protein's causality to an outcome.

129   Variable levels of the anti-inflammatory protein TREM2 were associated with two distinct

130   genomic regions (**Fig. 3a** and **Supplementary Fig. S3**). This included the missense variant

131   rs75932628 (NP_061838.1: p.R47H) in *TREM2* at chromosome 6 (**Fig. 3b**), known to confer

132   a strong risk of late-onset Alzheimer´s disease (LOAD)[27]. The variant was also associated

133   with IGFBPL1 (P = 3×10^{-18}) in serum (**Supplementary Table 1**), a protein recently

134   implicated in axonal growth[28]. Intriguingly, the region at chromosome 11 associated with

135   soluble TREM2 levels harbors variants adjacent to the genes *MS4A4A* and *MS4A6A* including

136   rs610932 known to influence genetic susceptibility for LOAD[29] (**Table 1** and **Fig. 3a**, **b**).

137   The variant rs610932 was also associated with the proteins GLTPD2 and A4GALT

138   (**Supplementary Table 1**). The alleles increasing risk of LOAD for both the common variant

139   rs610932 and the low-frequency variant rs75932628 were associated with low levels of

140   soluble TREM2 (**Fig. 3b**). Consistently, we find that the high-risk allele for rs75932628 was

141   associated with accelerated mortality post incident LOAD in the AGES-RS (**Fig. 3c**). It is of

142   note that the levels of TREM2 in the cerebrospinal fluid (CSF) reflect the activity of brain

143   TREM2-triggered microglia[4,30], while high levels of CSF TREM2 have been associated with

144   improved cognitive functioning[31]. **Supplementary Fig. S4** highlights the correlation

145   (Spearman rank) between the different proteins affected by the LOAD risk loci at

146   chromosomes 6 and 11. The accumulated data show a directionally consistent effect at

147   independent risk loci for LOAD converging on the same causal candidate TREM2.

148   Furthermore, a two-sample MR analysis using genetic instruments across the *TREM2* and

149   *MS4A4A/MS4A6A* loci and GWAS associations for LOAD in Europeans as outcome[32],

150   provided evidence that variable TREM2 protein levels are causally related to LOAD (P =

151   7.6×10^{-5}) (**Fig 3d**). In summary, these results demonstrate that the effect of genetic drivers on

152   major brain-linked disease like LOAD can be readily detected in serum to both inform on the

153   causal relationship and the directionality of the risk mediating effect. This would also suggest

154   that serum may be an accessible proxy for microglia function and cognition.

155   Variable levels of the cell adhesion protein SVEP1 are associated with variants located at

156   chromosomes 1 and 9 (**Supplementary Table 1**, **Fig. 4a** and **Supplementary Fig. S5**).

157   Genetic associations to SVEP1 levels at chromosome 9 include the low-frequency missense

158   variant rs111245230 in SVEP1 (NP_699197.3: pD2702G) (**Fig. 4b**), which was recently

159   linked to coronary heart disease (CHD), blood pressure and type-2-diabetes (T2D)[33]. Overall,

160   we found eight different missense mutations in *SVEP1* that were associated with SVEP1

161   serum levels (**Supplementary Table 1**). The CHD and T2D risk allele (C) of rs111245230

162   was associated with elevated levels of SVEP1, and SVEP1 levels were consistently elevated

163   in CHD and T2D patients (**Fig. 4c**). Furthermore, high SVEP1 levels were positively

164   correlated with systolic blood pressure ($\beta = 2.10$, $P = 4\times10^{-12}$) (**Fig. 4c**), but not with diastolic

165   blood pressure ($\beta = 0.115$, $P = 0.413$). Consistently, higher serum levels of SVEP1 were

166   associated with increased mortality post-incident CHD in the AGES-RS (HR = 1.27, P =

167   9×10^{-9}) (**Fig. 4d**). The variants at chromosome 1 linked to SVEP1 levels (**Fig. 4a**), have not

168   previously been linked to any disease. Given the currently available GWAS summary

169   statistics, a two-sample MR analysis using *cis*-variants on chromosome 9 for SVEP1 as

170   instruments and a GWAS associations for T2D[34] support a causal relationship of SVEP1 with

171   T2D ($P = 1.2\times10^{-5}$) (**Fig. 4e**), but not with CHD[35] or systolic blood pressure[36] ($P > 0.05$). Our

172   data triangulation and causal tests integrating genetics, serum protein levels and disease(s),

173   indicate that SVEP1 may be a therapeutic target for T2D.

174   The ILMN exome array contains several tags related to previous GWAS findings[37], including

175   many risk loci for cancer. For example, 21 loci associated with melanoma[38] and 50 loci

176   associated with colorectal cancer[39]. The exome array variant rs910873 located in an intron of

177   the GPI transamidase gene *PIGU* was previously linked to melanoma risk[40]. The reported

178   candidate gene *PIGU* is the gene most proximal to the lead SNP rs910873 and may be a novel

179   candidate gene involved in melanoma. However, a more biologically relevant candidate is the

180   agouti-signaling protein (*ASIP*) gene that is located 314kb downstream of the lead SNP

181   rs910873. *ASIP* is a competitive inhibitor of MC1R[41], and is thus strongly biologically

182   implicated in melanoma risk[42]. We found that the melanoma risk allele for rs910873 was

183   associated with elevated ASIP serum levels (P = 3×10^{-179}) and the variant had no effect on

184   other proteins measured with the current proteomic platform (**Fig. 5a**, **Supplementary Table**

185   **1** and **Table 1**). Interestingly, the pQTL rs910873 is also an eQTL for *ASIP* gene expression

186   in skin[43], showing directionally consistent effect on the mRNA and protein. Importantly, we

187   found that serum ASIP levels were supported as causally related to malignant melanoma (P =

188   4.8×10^{-26}) using a two-sample MR analysis on the protein-to-outcome causal sequence of

189   events (**Fig. 5b**). Our data point to the ASIP protein underlying the risk at rs910873, thus

190   providing supportive evidence for the hypothesis that ASIP mediated inhibition of MC1R

191   results in suppression of melanogenesis and increased risk of melanoma[44]. An additional

192   example is the susceptibility variant rs1800469 for colorectal cancer[45], which is a proxy to the

193   pQTL rs2241714 (r^2=0.978) (**Table 1** and **Fig. 5b**). While the *TMEM91* gene was the

194   reported candidate gene for the colorectal cancer risk at the rs1800469 (**Table 1**), we find that

195   the risk variant affected three proteins in either *cis* (B3GNT8 and TGFB1) or *trans* (B3GNT2)

196   (**Fig. 5b**). Intriguingly, all three proteins have previously been implicated in colorectal

197   cancer[46-48]. Due to a lack of available and powered GWAS summary statistics data, we were

198   unable to formally test the causality of these proteins to colorectal cancer. In conclusion,

199   while we cannot rule out *PIGU* as a candidate gene for malignant melanoma, these findings

200   point to an alternate, and possibly more biologically relevant, candidate, ASIP.

201   We outlined the construction of the serum protein network in our previous report and

202   identified common genetic variants underlying the network structure[10]. This included a

203   targeted study of the effects of common *cis* and *cis*-to-*trans* acting variants on levels of serum

204   proteins. The comparison between that study and the current one using all independent study-

205   wide signficiant associations (**Supplementary Table S2**) and linkage disequilibrium (LD)

206   threshold of r^2>0.50 for known associations, shows that 77.2% of the current study's variant-to-

207   protein associations are novel. Importantly, while 70% of the variants detected with the

208   exome array are exonic and 59% of mapped pQTLs in the current study are exonic, only 7%

209   of the identified pQTLs were exonic in our earlier report[10]. Previously, we discovered that

210   80% of *cis* pQTL effects and 74% of *trans* pQTL effects were replicated across populations

211   and proteomics platforms measuring common variants[10]. Given that the exome array platform

212   is enriched for rare and low-frequency variants, a comparable test of replication is not

213   straightforward. Examining the proteins and variants measured across studies, we find that

214   76.0% of SNP-to-protein associations are novel in the present study when compared to, say,

215   Sun et al.[11], and 60.1% are novel when compared to the majority of studies published to date

216   (**Supplementary Table S5**), for all independent associations in the current study and LD of

217   r^2<0.5 between study specific markers.

218   We report here that many of the measured serum proteins under genetic control share genetics

219   with a variety of clinical features, including major diseases arising from various body tissues.

220   This is in line with a recent population-scale survey of human induced pluripotent stem cells,

221   demonstrating that pQTLs are 1.93-fold enriched in disease risk variants compared to a 1.36-

222   fold enrichment for eQTLs[12], underscoring the added value in pQTL mapping. We reaffirm

223   widespread associations between genetic variants and their cognate proteins as well as distant

224   *trans*-acting effects on serum proteins and demonstrate that many proteins are often involved

225   in mediating the biological effect of a single causal variant affecting complex disease. Protein

226   coding variants may cause technical artifacts in both affinity proteomics and mass

227   spectrometry[49,50]. Systematic conditional and colocalization studies have shown, however,

228   that pQTLs powered by common missense variants being artifactual are not a common event

229   using the aptamer-based technology[11,51], however, given the enrichment of missense variants

230   in the present study, it may occur in some cases.

231   We note that with the ever-increasing availability of large-scale omics data aligned with the

232   human genome, cross-referencing different datasets can result in findings that occurred by

233   sheer chance. Hence, a systematic colocalization analysis has been proposed for identifying

234   shared causal variants between intermediate traits and disease endpoints[52]. This is, however,

235   not feasible for application of the exome array given its sparse genomic coverage. Instead,

236   multi-omics data triangulation to infer consistency in directionality, the approach used in the

237   present study, can enhance confidence in the causal call and offer insights and guidelines for

238   experimental follow-up studies. In fact, the causal calls for TREM2 (LOAD), SVEP1 (T2D)

239   and ASIP (melanoma) were validated, using a two-sample MR analysis. We previously

240   asserted that serum proteins are intimately connected to and may mediate global

241   homeostasis[10]. The accumulated data show that serum proteins are under strong genetic

242   control and closely associated with diseases of different aetiologies, which in turn suggests

243   that serum proteins may be significant mediators of systemic homeostasis in human health

244   and disease.

METHODS

Study population

247   Participants aged 66 through 96 are from the Age, Gene/Environment Susceptibility

248   Reykjavik Study (AGES-RS) cohort[53]. AGES-RS is a single-center prospective population-

249   based study of deeply phenotyped subjects (5764, mean age 75±6 years) and survivors of the

250   40-year-long prospective Reykjavik study (n~18,000), an epidemiologic study aimed to

251   understand aging in the context of gene/environment interaction by focusing on four biologic

252   systems: vascular, neurocognitive (including sensory), musculoskeletal, and body

253   composition/metabolism. Descriptive statistics of this cohort as well as detailed definition of

254   the various disease endpoints and relevant phenotypes measured have been published[10,53]. The

255   AGES-RS was approved by the NBC in Iceland (approval number VSN-00-063), and by the

256   National Institute on Aging Intramural Institutional Review Board, and the Data Protection

257   Authority in Iceland.

258   **Genotyping platform**

259   Genotyping was conducted using the exome-wide genotyping array Illumina HumanExome-

260   24 v1.1 Beadchip from Illumina (San Diego, CA, USA) for all AGES-RS participants as

261   previously described[54]. The exome array was enriched for exonic variants selected from over

262   12,000 individual exome and whole-genome sequences from different study populations[37],

263   and includes as well tags for previously described GWAS hits, ancestry informative markers,

264   mitochondrial SNPs and human leukocyte antigen tags[37]. A total of 244,883 variants were

265   included on the exome array. Genotype call and quality control filters including call rate,

266   heterozygosity, sex discordance and PCA outliers were performed as previously described[2,21].

267   Variants with call rate <90% or with Hardy–Weinberg P values $<1\times10^{-7}$ were removed from

268   the study. 72,766 variants were detected in at least one individual of the AGES-RS cohort. Of

269   these variants, 54,469 had a minor allele frequency > 0.001 and were examined for

270   association against each of the 4782 human serum protein measurements (see below).

271   **Protein measurements**

272   Each protein has its own detection reagent selected from chemically modified DNA libraries,

273   referred to as Slow Off-rate Modified Aptamers (SOMAmers)[55]. The design and quality

274   control of the SOMApanel platform's custom version to include proteins known or predicted

275   to be present in the extracellular milieu have been described in detail elsewhere[10]. Briefly

276   though, the aptamer-based platform measures 5034 protein analytes in a single serum sample,

277   of which 4782 SOMAmers bind specifically to 4137 human proteins (some proteins are

278   identified by more than one aptamer) and 250 SOMAmers that recognize non-human targets

279   (47 non-human vertebrate proteins and 203 targeting human pathogens)[10]. Consistent target

280   specificity across the platform was indicated by direct (through mass spectrometry) and/or

281   indirect validation of the SOMAmers[10]. Both sample selection and sample processing for

282   protein measurements were randomized, and all samples were run as a single set to prevent

283   batch or time of processing biases.

284   **Statistical analysis**

285   Prior to the analysis of the proteins measurements, we applied a Box-Cox transformation on

286   all proteins to improve normality, symmetry and to maintain all protein variables on a similar

287   scale[56]. In the association analysis, we obtained residuals after controlling for sex, age,

288   potential population stratification using principal component (PCs) analysis[57], and for all

289   single-variant associations to serum proteins tested under an additive genetic model applying

290   linear regression analysis (protein ~ SNP + age + sex + PC1 + PC2 + ….PC5). We report both

291   variants to protein associations at $P < 1 \times 10^{-6}$ for suggestive evidence and Bonferroni

292   correction for multiple comparisons by adjusting for the 54,469 variants and 4782 human

293   protein analytes where single variant associations with $P < 1.9 \times 10^{-10}$ were considered study-

294   wide significant (**Supplementary Table S1**). P-values corresponding to the estimated effect

295   size and standard errors of the genotypes, were recalculated to increase accuracy. Independent

296   genetic signals were found through a stepwise conditional and joint association analysis for

297   each protein analyte separately with the GCTA-COJO software[58,59]. We conditioned on the

298   current lead variant listed in **Supplementary Table S1**, defined as the variant with the lowest

299   P-value, and then kept track of any new variants that were not in LD (the default GCTA-

300   COJO option $r^2 < 0.9$ for colinearity) with previously chosen lead variants and reported

301   findings at P-value $< 1 \times 10^{-6}$ (**Supplementary Table S2**). In the joint model all conditionally

302   significant SNPs for each protein analyte were combined in the regression model.

303   **Supplementary Table S3** summarizes, through use of VEP[24,25], various pathogenicity

304   prediction scores for all independent study-wide significant pQTLs in **Supplementary Table**

305   **S2**, including the Likelihood Ratio Test (LRT)[60], Variant Effect Scoring Tool (VEST)[61],

306   MutationAssessor[62] and MutationTaster[63]. To test whether the percentage of secreted proteins

307   among pQTLs is equal to the percentage of secreted proteins among non-pQTLs, 10,000

308   permutations were performed to obtain the empirical distribution of the χ^2 test of equality of

309   proportions. Our null and alternate hypotheses were:

310   H_0: P(pQTL | Secreted) = P(pQTL | Not Secreted) and H_1: P(pQTL | Secreted) > P(pQTL | Not Secreted)

311   The test statistics calculated from our data was compared to the quantiles of this distribution

312   to obtain P(Data|H_0) (**Supplementary Fig. S1**).

313   We applied the "TwoSampleMR" R package[64] to perform a two-sample MR analysis to test

314   for causal associations between protein and outcome (protein-to-outcome). For different

315   outcomes we used GWAS associations for LOAD in Europeans[32], malignant melanoma in

316   European individuals from the UK biobank data (UKB-b-12915)[65] and T2D in Europeans[34].

317   Genetic variants (SNPs) associated with serum protein levels at a genome-wide significant

318   threshold (P<5×10^{-8}) identified in the AGES dataset and filtered to only include uncorrelated

319   variants (r^2<0.2) were used as instruments. The inverse variance weighted (IVW) method[66]

320   was used for the MR analysis, with P-values < 0.05 considered significant.

321   For the associations of individual proteins to different phenotypic measures we used linear or

322   logistic regression or Cox proportional hazards regression, depending on the outcome being

323   continuous, binary or a time to an event. Given consistency in terms of sample handling

324   including time from blood draw to processing (between 9-11 am), same personnel handling

325   all specimens and the ethnic homogeneity of the population we adjusted only for age and sex

326   in all our regression analyses. All statistical analysis was performed using R version 3.6.0 (R

327   Foundation for Statistical Computing, Vienna, Austria).

328 We compared our pQTL results to 19 previously published proteogenomic studies

329 (**Supplementary Table 5**), including the protein GWAS in the INTERVAL study[11], and our

330 previously reported genetic analysis of 3,219 AGES cohort participants[10]. In the previous

331 proteogenomic analysis of AGES participants, one *cis* variant was reported per protein using a

332 locus-wide significance threshold, as well as *cis*-to-*trans* variants at a Bonferroni corrected

333 significance threshold. Due to these differences in reporting criteria, we only considered the

334 associations in previous AGES results that met the current study-wide P-value threshold. For

335 all other studies we retained the pQTLs at the reported significance threshold. In addition, we

336 performed a lookup of all independent pQTLs from the current study available in summary

337 statistics from the INTERVAL study, considering them known if they reached a study-wide

338 significance in their data. We calculated the LD structure between the reported significant

339 variants for all studies, using 1000 Genomes v3 EUR samples, but using AGES data when

340 comparing to previously reported AGES results. We considered variants in LD at $r^2>0.5$ to

341 represent the same signal across studies. Comparison was performed on protein level, by

342 matching the reported Entrez gene symbol from each study.

Acknowledgements

350

351

References

1   Buniello, A. *et al.* The NHGRI-EBI GWAS Catalog of published genome-wide association studies, targeted arrays and summary statistics 2019. *Nucleic Acids Research* **47**, D1005-D1012, doi:10.1093/nar/gky1120 (2019).

2   Liu, D. J. *et al.* Exome-wide association study of plasma lipids in >300,000 individuals. *Nature Genetics* **49**, 1758-1766, doi:10.1038/ng.3977 (2017).

3   Schadt, E. E. Molecular networks as sensors and drivers of common human diseases. *Nature* **461**, 218-223, doi:10.1038/nature08454 (2009).

4   Zhang, B. *et al.* Integrated Systems Approach Identifies Genetic Nodes and Networks in Late-Onset Alzheimer's Disease. *Cell* **153**, 707-720, doi:10.1016/j.cell.2013.03.030 (2013).

5   Emilsson, V. *et al.* Genetics of gene expression and its effect on disease. *Nature* **452**, 423-U422, doi:10.1038/nature06758 (2008).

6   Chen, Y. Q. *et al.* Variations in DNA elucidate molecular networks that cause disease. *Nature* **452**, 429-435, doi:10.1038/nature06757 (2008).

7   Pires, D. E., Chen, J., Blundell, T. L. & Ascher, D. B. In silico functional dissection of saturation mutagenesis: Interpreting the relationship between phenotypes and changes in protein stability, interactions and activity. *Sci Rep* **6**, 19848, doi:10.1038/srep19848 (2016).

8   Ho, J. E. *et al.* Common genetic variation at the IL1RL1 locus regulates IL-33/ST2 signaling. *Journal of Clinical Investigation* **123**, 4208-4218, doi:10.1172/JCI67119 (2013).

9   Interleukin-6 Receptor Mendelian Randomisation Analysis, C. *et al.* The interleukin-6 receptor as a target for prevention of coronary heart disease: a mendelian randomisation analysis. *Lancet* **379**, 1214-1224, doi:10.1016/s0140-6736(12)60110-x (2012).

10   Emilsson, V. *et al.* Co-regulatory networks of human serum proteins link genetics to disease. *Science* **361**, 769-773, doi:10.1126/science.aaq1327 (2018).

11   Sun, B. B. *et al.* Genomic atlas of the human plasma proteome. *Nature* **558**, 73-79, doi:10.1038/s41586-018-0175-2 (2018).

12   Mirauta, B. A. *et al.* Population-scale proteome variation in human induced pluripotent stem cells. *Elife* **9**, doi:10.7554/eLife.57390 (2020).

13   Lamb, J. R., Jennings, L. L., Gudmundsdottir, V., Gudnason, V. & Emilsson, V. It's in Our Blood: A Glimpse of Personalized Medicine. *Trends Mol Med*, doi:10.1016/j.molmed.2020.09.003 (2020).

14   Emilsson, V., Gudnason, V. & Jennings, L. L. Predicting health and life span with the deep plasma proteome. *Nat Med* **25**, 1815-1816, doi:10.1038/s41591-019-0677-y (2019).

15   Lehallier, B. *et al.* Undulating changes in human plasma proteome profiles across the lifespan. *Nat Med* **25**, 1843-1850, doi:10.1038/s41591-019-0673-2 (2019).

16   Williams, S. A. *et al.* Plasma protein patterns as comprehensive indicators of health. *Nat Med* **25**, 1851-1857, doi:10.1038/s41591-019-0665-2 (2019).

17   Nakamura, A. *et al.* High performance plasma amyloid-beta biomarkers for Alzheimer's disease. *Nature* **554**, 249-254, doi:10.1038/nature25456 (2018).

18   Dodgson, S. E. There Will Be Blood Tests. *Cell* **173**, 1-3, doi:10.1016/j.cell.2018.03.012 (2018).

19   Cohen, J. D. *et al.* Detection and localization of surgically resectable cancers with a multi-analyte blood test. *Science* **359**, 926-930, doi:10.1126/science.aar3247 (2018).

20   Kristensen, S. L. *et al.* Prognostic Value of N-Terminal Pro-B-Type Natriuretic Peptide Levels in Heart Failure Patients With and Without Atrial Fibrillation. *Circ Heart Fail* **10**, doi:10.1161/circheartfailure.117.004409 (2017).

21   Peloso, G. M. *et al.* Association of low-frequency and rare coding-sequence variants with blood lipids and coronary heart disease in 56,000 whites and blacks. *American Journal of Human Genetics* **94**, 223-232, doi:10.1016/j.ajhg.2014.01.009 (2014).

22   Richards, A. L. *et al.* Exome arrays capture polygenic rare variant contributions to schizophrenia. *Human Molecular Genetics* **25**, 1001-1007, doi:10.1093/hmg/ddv620 (2016).

23   Armengaud, J., Christie-Oleza, J. A., Clair, G., Malard, V. & Duport, C. Exoproteomics: exploring the world around biological systems. *Expert Rev Proteomics* **9**, 561-575, doi:10.1586/epr.12.52 (2012).

24   McLaren, W. *et al.* The Ensembl Variant Effect Predictor. *Genome Biol* **17**, 122, doi:10.1186/s13059-016-0974-4 (2016).

25   McLaren, W. *et al.* Deriving the consequences of genomic variants with the Ensembl API and SNP Effect Predictor. *Bioinformatics* **26**, 2069-2070, doi:10.1093/bioinformatics/btq330 (2010).

26   Staley, J. R. *et al.* PhenoScanner: a database of human genotype-phenotype associations. *Bioinformatics* **32**, 3207-3209, doi:10.1093/bioinformatics/btw373 (2016).

27   Jonsson, T. *et al.* Variant of TREM2 associated with the risk of Alzheimer's disease. *N Engl J Med* **368**, 107-116, doi:10.1056/NEJMoa1211103 (2013).

28   Guo, C. *et al.* IGFBPL1 Regulates Axon Growth through IGF-1-mediated Signaling Cascades. *Sci Rep* **8**, 2054, doi:10.1038/s41598-018-20463-5 (2018).

29   Hollingworth, P. *et al.* Common variants at ABCA7, MS4A6A/MS4A4E, EPHA1, CD33 and CD2AP are associated with Alzheimer's disease. *Nature Genetics* **43**, 429-435, doi:10.1038/ng.803 (2011).

30   Suarez-Calvet, M. *et al.* sTREM2 cerebrospinal fluid levels are a potential biomarker for microglia activity in early-stage Alzheimer's disease and associate with neuronal injury markers. *EMBO Mol Med* **8**, 466-476, doi:10.15252/emmm.201506123 (2016).

31   Ewers, M. *et al.* Increased soluble TREM2 in cerebrospinal fluid is associated with reduced cognitive and clinical decline in Alzheimer's disease. *Sci Transl Med* **11** (2019).

32   Kunkle, B. W. *et al.* Genetic meta-analysis of diagnosed Alzheimer's disease identifies new risk loci and implicates Aβ, tau, immunity and lipid processing. *Nat Genet* **51**, 414-430, doi:10.1038/s41588-019-0358-2 (2019).

33   Myocardial Infarction, G. *et al.* Coding Variation in ANGPTL4, LPL, and SVEP1 and the Risk of Coronary Disease. *N Engl J Med* **374**, 1134-1144, doi:10.1056/NEJMoa1507652 (2016).

34   Mahajan, A. *et al.* Fine-mapping type 2 diabetes loci to single-variant resolution using high-density imputation and islet-specific epigenome maps. *Nat Genet* **50**, 1505-1513, doi:10.1038/s41588-018-0241-6 (2018).

35   Nikpay, M. *et al.* A comprehensive 1,000 Genomes-based genome-wide association meta-analysis of coronary artery disease. *Nat Genet* **47**, 1121-1130, doi:10.1038/ng.3396 (2015).

36   Evangelou, E. *et al.* Genetic analysis of over 1 million people identifies 535 new loci associated with blood pressure traits. *Nat Genet* **50**, 1412-1425, doi:10.1038/s41588-018-0205-x (2018).

448 37 Huyghe, J. R. *et al.* Exome array analysis identifies new loci and low-frequency
449 variants influencing insulin processing and secretion. *Nature Genetics* **45**, 197-201,
450 doi:10.1038/ng.2507 (2013).
451 38 Ransohoff, K. J. *et al.* Two-stage genome-wide association study identifies a novel
452 susceptibility locus associated with melanoma. *Oncotarget* **8**, 17586-17592,
453 doi:10.18632/oncotarget.15230 (2017).
454 39 Lu, Y. *et al.* Large-Scale Genome-Wide Association Study of East Asians Identifies
455 Loci Associated With Risk for Colorectal Cancer. *Gastroenterology*,
456 doi:10.1053/j.gastro.2018.11.066 (2018).
457 40 Brown, K. M. *et al.* Common sequence variants on 20q11.22 confer melanoma
458 susceptibility. *Nature Genetics* **40**, 838-840, doi:10.1038/ng.163 (2008).
459 41 Blanchard, S. G. *et al.* Agouti antagonism of melanocortin binding and action in the
460 B16F10 murine melanoma cell line. *Biochemistry* **34**, 10406-10411 (1995).
461 42 Taylor, N. J. *et al.* Inherited variation at MC1R and ASIP and association with
462 melanoma-specific survival. *Int J Cancer* **136**, 2659-2667, doi:10.1002/ijc.29317
463 (2015).
464 43 Aguet, F. *et al.* The GTEx Consortium atlas of genetic regulatory effects across human
465 tissues. *bioRxiv*, 787903, doi:10.1101/787903 (2019).
466 44 Wolf Horrell, E. M., Boulanger, M. C. & D'Orazio, J. A. Melanocortin 1 Receptor:
467 Structure, Function, and Regulation. *Front Genet* **7**, 95, doi:10.3389/fgene.2016.00095
468 (2016).
469 45 Zhang, B. *et al.* Large-scale genetic study in East Asians identifies six new loci
470 associated with colorectal cancer risk. *Nature Genetics* **46**, 533-542,
471 doi:10.1038/ng.2985 (2014).
472 46 Calon, A. *et al.* Dependency of colorectal cancer on a TGF-beta-driven program in
473 stromal cells for metastasis initiation. *Cancer Cell* **22**, 571-584,
474 doi:10.1016/j.ccr.2012.08.013 (2012).
475 47 Venkitachalam, S. *et al.* Biochemical and functional characterization of glycosylation-
476 associated mutational landscapes in colon cancer. *Sci Rep* **6**, 23642,
477 doi:10.1038/srep23642 (2016).
478 48 Ishida, H. *et al.* A novel beta1,3-N-acetylglucosaminyltransferase (beta3Gn-T8),
479 which synthesizes poly-N-acetyllactosamine, is dramatically upregulated in colon
480 cancer. *Febs Letters* **579**, 71-78, doi:10.1016/j.febslet.2004.11.037 (2005).
481 49 Solomon, T. *et al.* Identification of Common and Rare Genetic Variation Associated
482 With Plasma Protein Levels Using Whole-Exome Sequencing and Mass Spectrometry.
483 *Circ Genom Precis Med* **11**, e002170, doi:10.1161/circgen.118.002170 (2018).
484 50 Smith, J. G. & Gerszten, R. E. Emerging Affinity-Based Proteomic Technologies for
485 Large-Scale Plasma Profiling in Cardiovascular Disease. *Circulation* **135**, 1651-1664,
486 doi:10.1161/circulationaha.116.025446 (2017).
487 51 Zheng, J. *et al.* Phenome-wide Mendelian randomization mapping the influence of the
488 plasma proteome on complex diseases. *bioRxiv*, 627398, doi:10.1101/627398 (2019).
489 52 Liu, B., Gloudemans, M. J., Rao, A. S., Ingelsson, E. & Montgomery, S. B. Abundant
490 associations with gene expression complicate GWAS follow-up. *Nature Genetics* **51**,
491 768-769, doi:10.1038/s41588-019-0404-0 (2019).
492 53 Harris, T. B. *et al.* Age, Gene/Environment Susceptibility-Reykjavik Study:
493 multidisciplinary applied phenomics. *Am J Epidemiol* **165**, 1076-1087,
494 doi:10.1093/aje/kwk115 (2007).
495 54 Grove, M. L. *et al.* Best practices and joint calling of the HumanExome BeadChip: the
496 CHARGE Consortium. *PLoS One* **8**, e68095, doi:10.1371/journal.pone.0068095
497 (2013).

498 55 Candia, J. *et al.* Assessment of Variability in the SOMAscan Assay. *Sci Rep* **7**, 14248,
499   doi:10.1038/s41598-017-14755-5 (2017).
500 56 Max Kuhn, K. J. *Applied Predictive Modeling*. (Springer, 2013).
501 57 Price, A. L. *et al.* Principal components analysis corrects for stratification in genome-
502   wide association studies. *Nat Genet* **38**, 904-909, doi:10.1038/ng1847 (2006).
503 58 Yang, J. *et al.* Conditional and joint multiple-SNP analysis of GWAS summary
504   statistics identifies additional variants influencing complex traits. *Nat Genet* **44**, 369-
505   375, s361-363, doi:10.1038/ng.2213 (2012).
506 59 Yang, J., Lee, S. H., Goddard, M. E. & Visscher, P. M. GCTA: a tool for genome-
507   wide   complex   trait   analysis.   *Am   J   Hum   Genet*   **88**,   76-82,
508   doi:10.1016/j.ajhg.2010.11.011 (2011).
509 60 Chun, S. & Fay, J. C. Identification of deleterious mutations within three human
510   genomes. *Genome Res* **19**, 1553-1561, doi:10.1101/gr.092619.109 (2009).
511 61 Carter, H., Douville, C., Stenson, P. D., Cooper, D. N. & Karchin, R. Identifying
512   Mendelian disease genes with the variant effect scoring tool. *BMC Genomics* **14**
513   **Suppl 3**, S3, doi:10.1186/1471-2164-14-s3-s3 (2013).
514 62 Reva, B., Antipin, Y. & Sander, C. Predicting the functional impact of protein
515   mutations: application   to   cancer   genomics.   *Nucleic   Acids   Res*   **39**,   e118,
516   doi:10.1093/nar/gkr407 (2011).
517 63 Schwarz, J. M., Rödelsperger, C., Schuelke, M. & Seelow, D. MutationTaster
518   evaluates disease-causing potential of sequence alterations. *Nat Methods* **7**, 575-576,
519   doi:10.1038/nmeth0810-575 (2010).
520 64 Hemani, G. *et al.* The MR-Base platform supports systematic causal inference across
521   the human phenome. *Elife* **7**, doi:10.7554/eLife.34408 (2018).
522 65 Sudlow, C. *et al.* UK biobank: an open access resource for identifying the causes of a
523   wide range of complex diseases of middle and old age. *PLoS Med* **12**, e1001779,
524   doi:10.1371/journal.pmed.1001779 (2015).
525 66 Burgess, S., Butterworth, A. & Thompson, S. G. Mendelian randomization analysis
526   with multiple genetic variants using summarized data. *Genet Epidemiol* **37**, 658-665,
527   doi:10.1002/gepi.21758 (2013).
528 67 MacArthur, J. *et al.* The new NHGRI-EBI Catalog of published genome-wide
529   association studies (GWAS Catalog). *Nucleic Acids Research* **45**, D896-D901,
530   doi:10.1093/nar/gkw1133 (2017).

531

Table 1 | Selected examples of exome array variants affecting serum protein levels and complex disease. CHD, coronary heart disease; VTE, venous thromboembolism; CKD, chronic kidney disease; T2D, type 2 diabetes; VAT, visceral adipose tissue; LOAD, late-onset Alzheimer´s disease; SLE, systemic lupus erythematous; IBD, inflammatory bowel disease; AMD, age-related macular degeneration; N/A, not applicable. All reported effects are genome-wide significant at $P < 1.92 \times 10^{-10}$.

Disease class	Disease trait	PMID or database	pQTL	GWAS lead SNP(s)[a]	Function pSNP[b]	Mapped GWAS locus[c]	#Proteins affected	Example of cis and/or trans affected proteins[d]
Cardiovascular								
	CHD	28714975	rs12740374	rs12740374	3'-UTR	CELSR2	8	**C1QTNF1, IGFBP1**
	VTE	UKBB, 28373160	rs2343596	rs16873402, rs4602861	Intron	ZFPM2	7	**VEGFA, DKK1**
	Stroke	26708676	rs653178	rs653178	Intron	ATXN2	2	**THPO, CXCL11**
Metabolic								
	T2D	22885922	rs7202877	rs7202877	Intergenic	CTRB1	5	CTRB1, **PRSS2, CPB1**
	VAT	20935629	rs9491696	rs9491696	Intron	RSPO3	1	RSPO3
	Triglyceride	21386085	rs2266788	rs2266788	3'-UTR	APOA5	5	APOA5, PCSK7, **ANGPTL3**
CNS								
	LOAD	21460840	rs610932	rs610932	3'-UTR	MS4A6A	3	**TREM2, GLTPD2**
	Parkinson	21738487	rs6599389	rs6599389	Intron	GAK	1	IDUA
	Schizophrenia	25056061	rs3617	rs3617	Q315K	ITIH3	8	ITIH3, **JAKMIP3**
Inflammatory								
	SLE, T1D	26502338	rs2304256	rs2304256	V362F	TYK2	2	ICAM1, ICAM5
	Crohn´s, IBD	21102463	rs11209026	rs11209026	R381Q	IL23R	1	IL23R
	AMD	2355636	rs10737680	rs10737680	Intron	CFH	22	CFH, CFHR1, **CFB**
Cancer								
	Colorectal	24836286	rs2241714	rs1800469	I11M	TMEM91	3	**B3GNT2**, TGFB1
	Lung	18978787	rs3117582	rs3117582	Intron	APOM	10	MICB, **ISG15**
	Melanoma	18488026	rs910873	rs910873	Intron	PIGU	1	ASIP

[a]Protein QTLs overlapping GWAS lead SNPs using the PhenoScanner database[23]. No SNP proxies were applied except when the lead pSNP was not in the query then we used the best proxy ($r^2 \geq 0.8$ between markers). [b]The functional annotation of pQTLs was obtained from the PhenoScanner database[23]. [c]Reported causal candidates are from the GWAS Catalog[67]. [d]The definition of *cis* vs. *trans* effects is somewhat arbitrary depending on the window size chosen across the protein gene in question. However, all affected proteins located at other chromosomes than the pQTL location, were considered *trans* acting and are highlighted in bold letters. All significant pQTLs are listed in Supplementary Table 1 and the overlap with GWAS risk loci summarized in Supplementary Table 4.
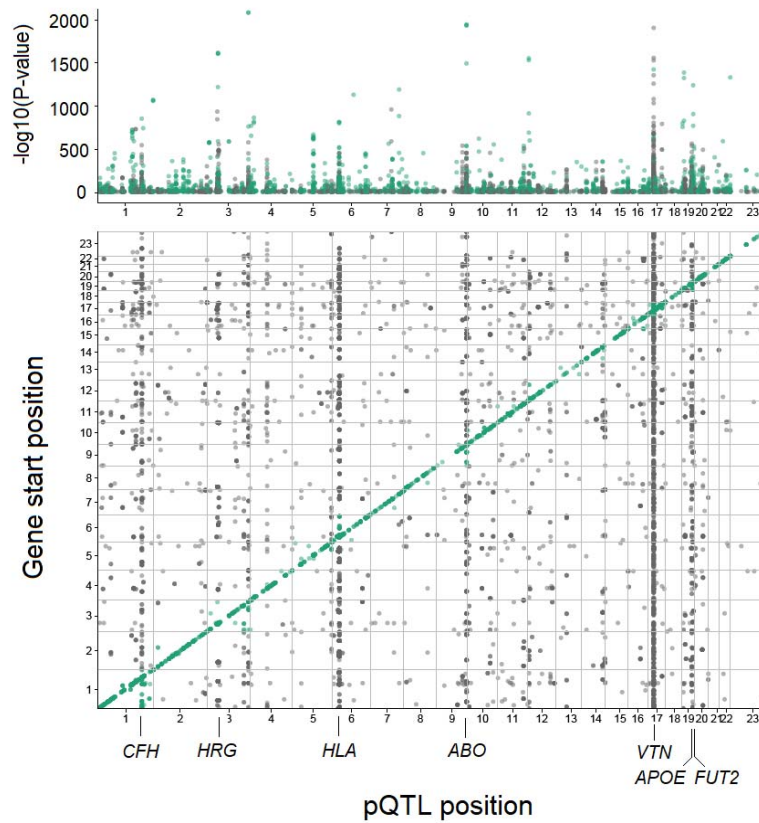
a
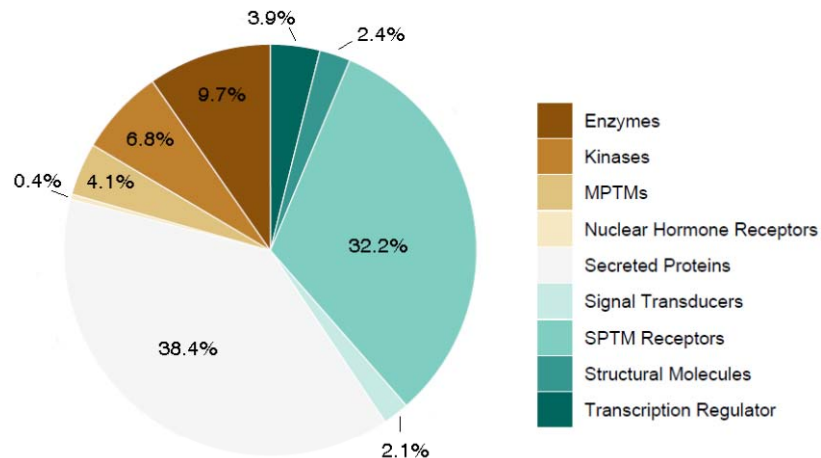
b

Fig. 1. Classification of the target protein population and genomic locations of observed pQTLs. a. Pie chart showing the relative distribution (percentage) of the different protein classes targeted by the present proteomics platform, with secreted proteins (38.4%) and single

pass transmembrane (SPTM) receptors (32.2%) dominating the target protein population.

Protein classes were manually curated based on information from the SecTrans, Gene

Ontology (GO) and Swiss-Prot databases, and were composed of secreted proteins (e.g.

cytokines, adipokines, hormones, chemokines and growth factors), SPTM receptors (e.g.

tyrosine and serine/threonine kinase receptors), multi-pass transmembrane (MPTM) receptors

(e.g. GPCR, ion channels, transporters), enzymes (intracellular), kinases, nuclear hormone

receptors, structural molecules, transcriptional regulators and signal transducers. **b**. The

Manhattan plot in the top panel uses precise P-values to highlight all study-wide significant

associations in Supplementary Table S1. The bottom panel shows the genomic locations of all

study-wide significant pQTLs ($P < 1.92 \times 10^{-10}$), where the start position of the protein

encoding gene is shown on the y-axis and the location of the pSNP at the x-axis. *Cis* acting

effects, using a 300kb window, appear at the diagonal while *trans* acting pQTL effects

including *trans* hot spots show up off-diagonally. The genetic loci highlighted across the x-

axis are *trans*-acting hotspots.
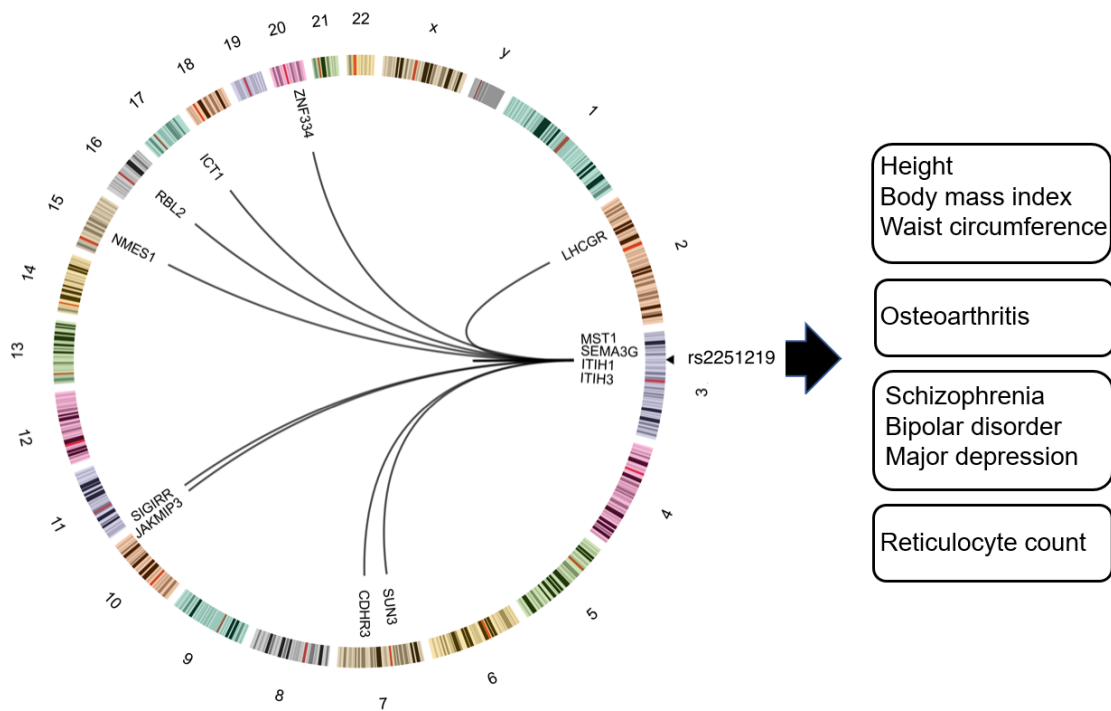
Fig. 2. **Pleiotropy of rs2251219 affecting many proteins and disease traits. a**. Circos plot showing the effect of the variant rs2251219 (Supplementary Tables 1 and 2) on 13 proteins acting in *cis* or *trans* and sharing genetics with various diseases of different etiologies. Only study-wide significant (P < 1.92 x 10^{-10}) genotype-to-protein associations are shown. Lines going from rs225121show links to genomic locations of the protein encoding genes affected while numbers refer to chromosomes.
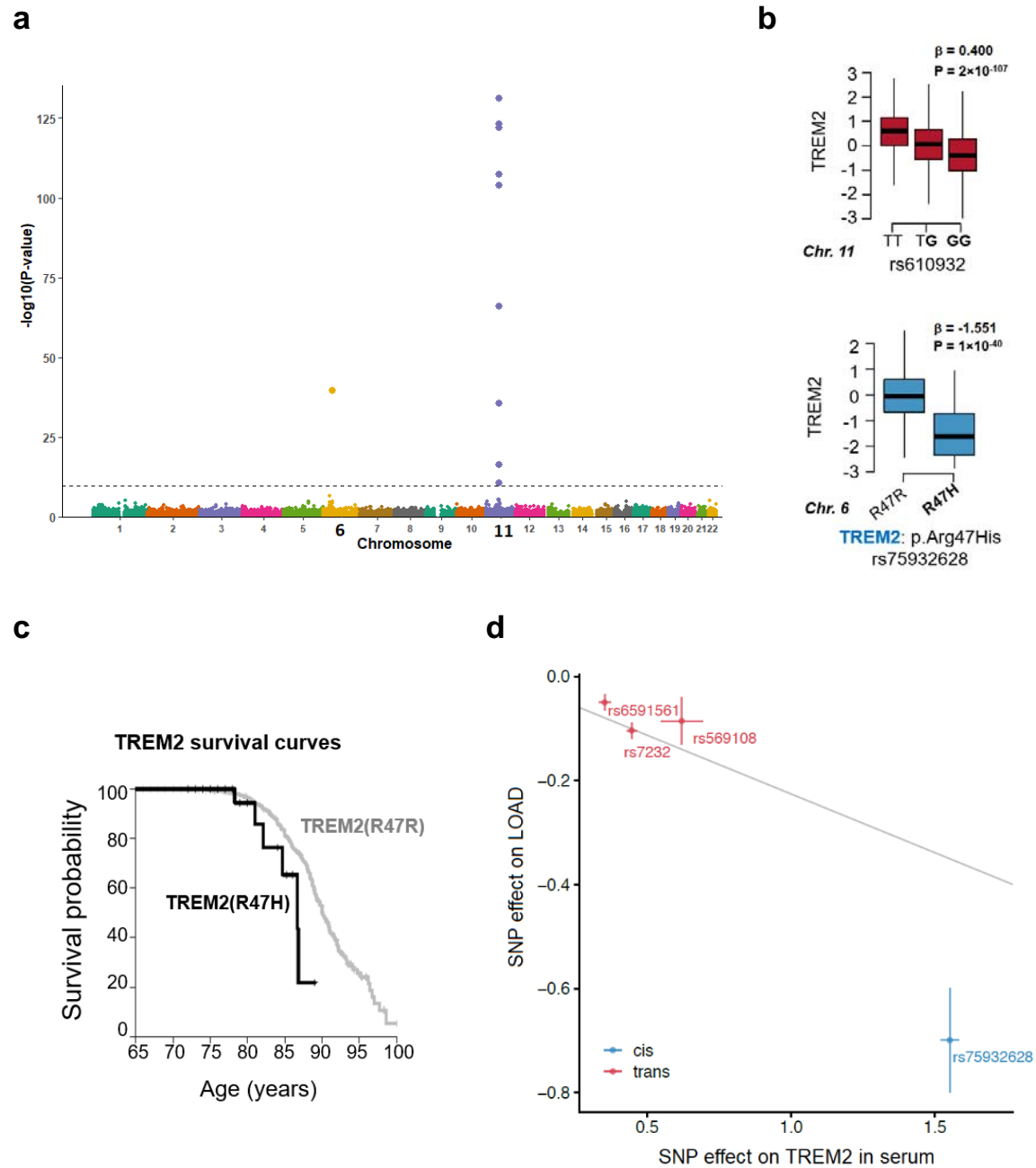
Fig. 3. Effects of distinct risk loci for LOAD converge on the protein TREM2. a. The

Manhattan plot highlights variants at two distinct chromosomes associated with serum

TREM2 levels. Study-wide significant associations at $P < 1.92 \times 10^{-10}$ are indicated by the

horizontal line. The y-axis shows the -($\log_{10}$) of the P-values for the association of each

genetic variant on the exome array present along the x-axis. Variants at both chromosomes 6

and 11 associated with TREM2 have been independently linked to risk of LOAD including the rs75932628 (NP_061838.1: p.R47H) in TREM2 at chromosome 6 and the variant rs610932 at chromosome 11. **b.** Boxplot of the *trans* effect of the well-established GWAS risk variant rs610932 for LOAD on TREM2 serum levels (upper panel), where the LOAD risk allele G (highlighted in bold) is associated with lower levels of TREM2. Similarly, the LOAD causing p.R47H mutation was associated with low levels of TREM2 (lower panel). **c.** TREM2p.R47H carriers demonstrated lower survival probability post-incident LOAD compared to TREM2p.R47R carriers (P = 0.04). **d.** Scatterplot for the TREM2 protein supported as having a causal effect on LOAD in a two sample MR analysis. The figure demonstrates the estimated effects (with 95% confidence intervals) of their respective *cis-* and *trans*-acting genetic instruments on the serum TREM2 levels in AGES-RS (x-axis) and risk of LOAD through a GWAS by Kunkle et al.[32] (y-axis), using 21,982 LOAD cases and 41,944 controls. The line indicates the inverse variance weighted causal estimate (β = -0.226, SE = 0.057, P = 7.6×10^{-5}).
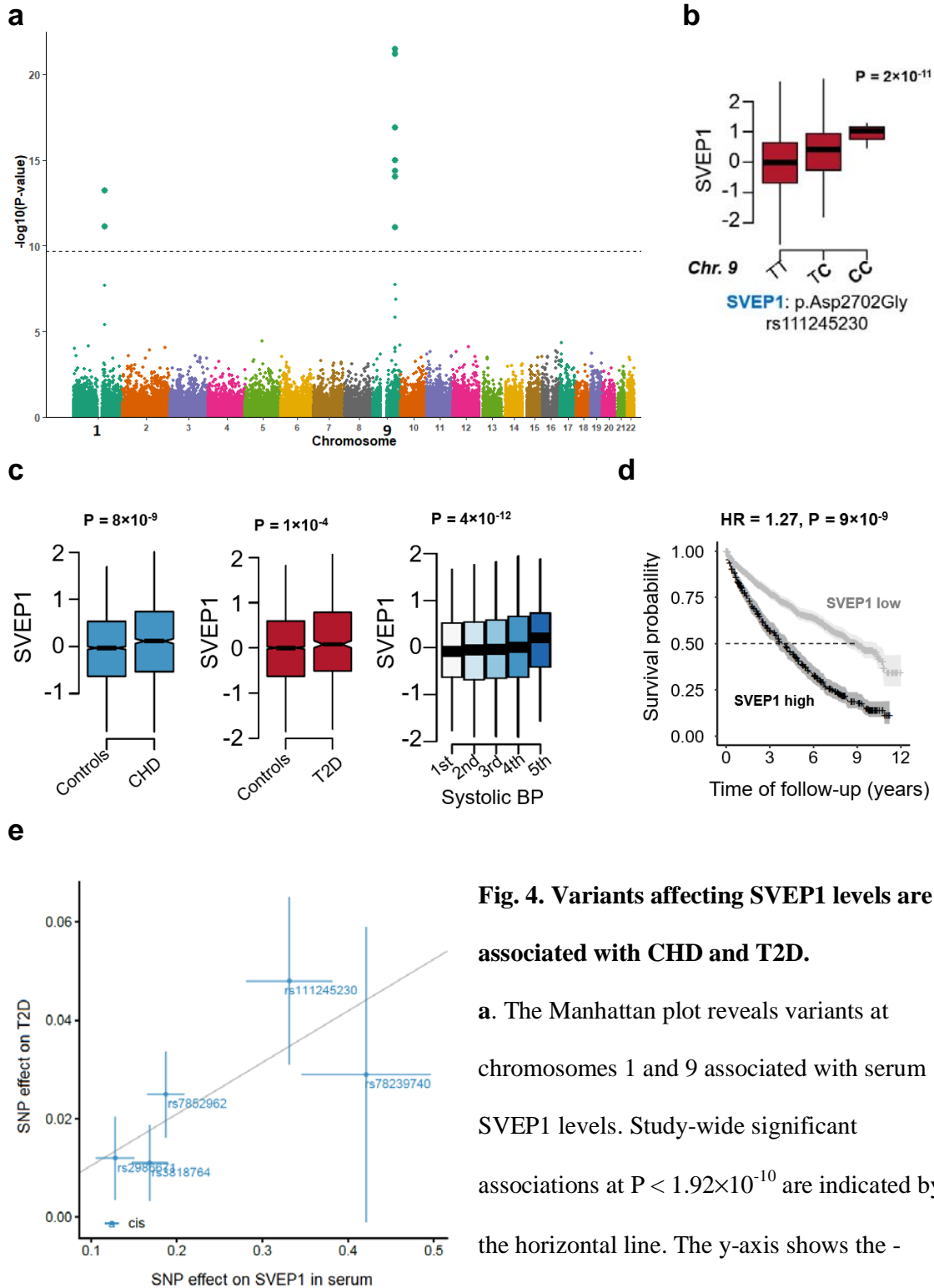
Fig. 4. Variants affecting SVEP1 levels are associated with CHD and T2D.

a. The Manhattan plot reveals variants at chromosomes 1 and 9 associated with serum SVEP1 levels. Study-wide significant associations at $P < 1.92×10^{-10}$ are indicated by the horizontal line. The y-axis shows the -($\log_{10}$) of the P-values for the association of each genetic variant on the exome array present along the x-axis. **b**. One of the variants associated with SVEP1 levels and underlying the peak at chromosome 9 is the low-frequency

CHD risk variant rs111245230 (NP_699197.3: pAsp2702Gly). The CHD risk allele C (highlighted in bold) is associated with increased serum SVEP1 levels. **c**. Serum levels of SVEP1 were associated with CHD ($P = 8 \times 10^{-9}$), T2D ($P = 1 \times 10^{-4}$) and systolic blood pressure ($P = 4 \times 10^{-12}$) in the AGES-RS, all in a directionally consistent manner. **d**. Consistent with the directionality of the effects described above, we find that elevated levels of SVEP1 were associated with higher rates of mortality post-incident CHD. **e**. Scatterplot for the SVEP1 protein supported as having a causal effect on T2D in a two-sample MR analysis. The figure demonstrates the estimated effects (with 95% confidence intervals) of the SNP effect on serum SVEP1 levels and T2D from a GWAS in Europeans[34] (y-axis), with 74,124 T2D patients and 824,006 controls. The line indicates the inverse variance weighted causal estimate ($\beta = 0.105$, $SE = 0.024$, $P = 1.2 \times 10^{-5}$).
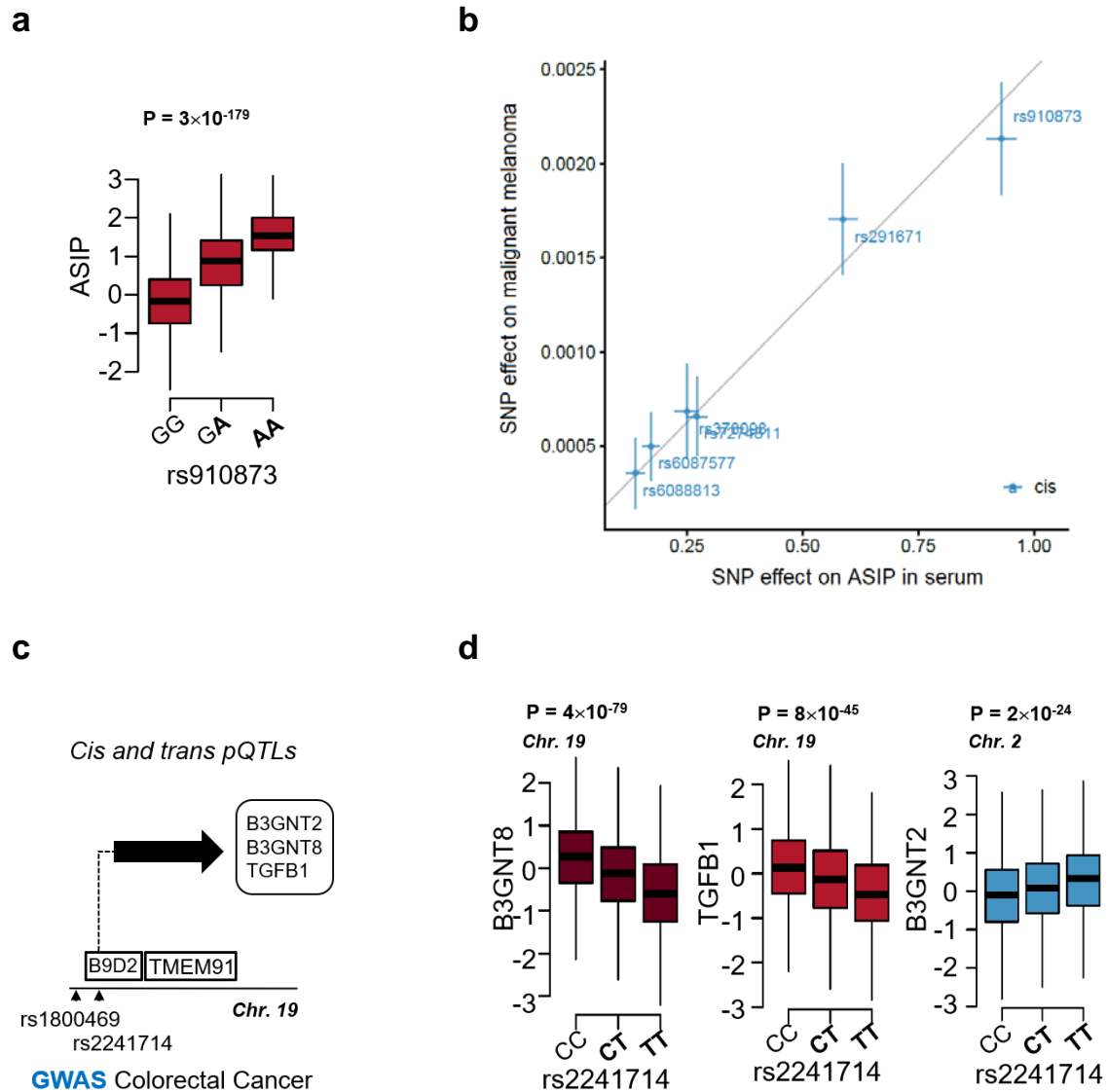
Figure 5. Proteins associated with malignant melanoma and colorectal cancer. **a**. The melanoma risk allele A (highlighted in bold) for the variant rs910873 is associated with high serum levels of ASIP. **b**. Scatterplot for the ASIP protein supported as having a causal effect on malignant melanoma in a two sample MR analysis. The figure demonstrates the estimated effects (with 95% confidence intervals) of their respective genetic instruments on the serum ASIP levels in AGES (x-axis) and risk of melanoma in GWAS by UK biobank data (UKB-b-12915) [65] (y-axis), that included 3598 melanoma cases and 459,335 controls. The line indicates the inverse variance weighted causal estimate ($\beta = 0.0025$, SE = 0.0002, P = $4.8 \times 10^-$

[26]). **c**. The pQTL rs2241714 is a proxy for the colorectal cancer associated variant rs1800469 ($r^2 = 0.978$) (Supplementary Table 2), located within the gene *B9D2* and proximal to *TMEM91* which is the reported candidate gene at this locus (see Table 1). **d**. The variant rs2241714 (and rs1800469) regulate three serum proteins, B3GNT2 (in *trans*), B3GNT8 (in *cis*) and TGFB1 (in *cis*).

SUPPLEMENTARY MATERIAL

Coding and regulatory variants affect serum protein levels and common disease

Valur Emilsson[1,2, ξ,*], Valborg Gudmundsdottir[1,ξ], Alexander Gudjonsson[1,ξ], Mohd A Karim[3,4], Marjan Ilkov[1], James R. Staley[5], Elias F. Gudmundsson[1], Brynjolfur G. Jonsson[1], Lenore J. Launer[6], Jan H. Lindeman[7], Nicholas M. Morton[8], Thor Aspelund[1], John R. Lamb[9], Lori L. Jennings[10] and Vilmundur Gudnason[1,2,*]

[1]Icelandic Heart Association, Holtasmari 1, IS-201 Kopavogur, Iceland.
[2]Faculty of Medicine, University of Iceland, 101 Reykjavik, Iceland
[3]Wellcome Trust Sanger Institute, Welcome Genome Campus, Hinxton, Cambridgeshire CB10 1SA, UK.
[4]Open Targets, Wellcome Genome Campus, Hinxton, Cambridgeshire CB10 1SD, UK
[5]MRC/BHF Cardiovascular Epidemiology Unit, Department of Public Health and Primary Care, University of Cambridge, Cambridge, UK
[6]Laboratory of Epidemiology and Population Sciences, Intramural Research Program, National Institute on Aging, Bethesda, MD 20892-9205, USA.
[7]Department of General Surgery Leiden University Medical Center, Leiden. Holland
[8]Centre for Cardiovascular Sciences, Queen's Medical Research Institute, University of Edinburgh, Edinburgh EH16 4TJ, UK
[9]GNF Novartis, 10675 John Jay Hopkins Drive, San Diego, CA 92121, USA.
[10]Novartis Institutes for Biomedical Research, 22 Windsor Street, Cambridge, MA 02139, USA.
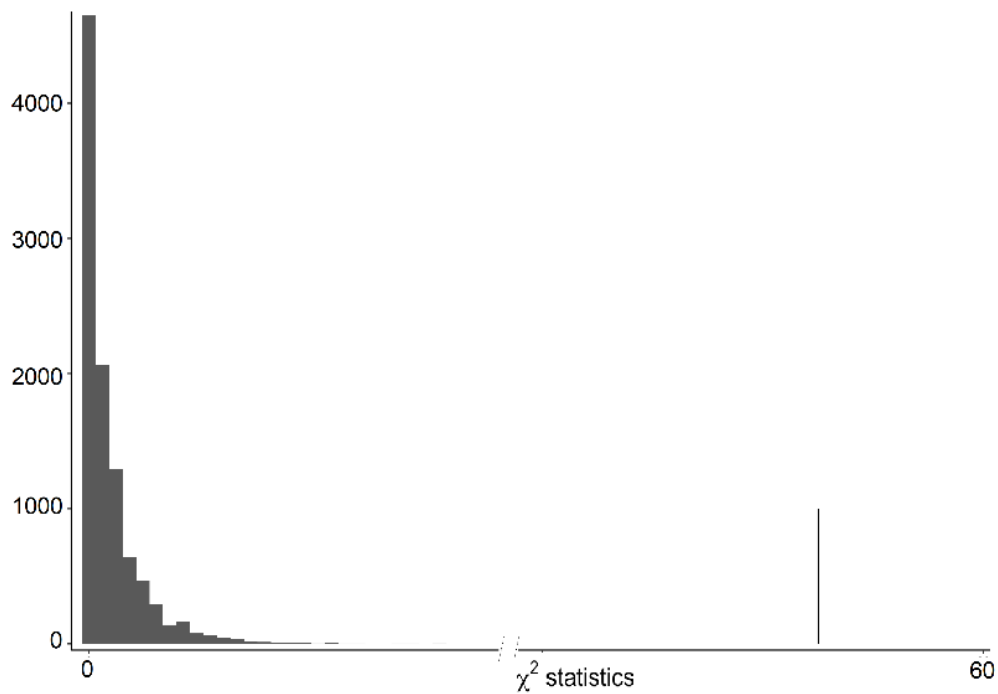
Supplementary Fig. S1. Empirical distribution of the test statistic as a histogram and the observed statistics calculated from our data as a vertical line. 10,000 permutations were performed to obtain the empirical distribution of the χ^2 test of equality of proportions of pQTLs among secreted versus non-secreted proteins. Here, the test statistics calculated from our data to the quantiles of this distribution to obtain $P(\text{Data}|H_0)$ were compared. Of 10,000 permutations none gave a value greater than the observed statistic leading us to P-value = $P(\text{Data}|H_0) < 0.0001$.
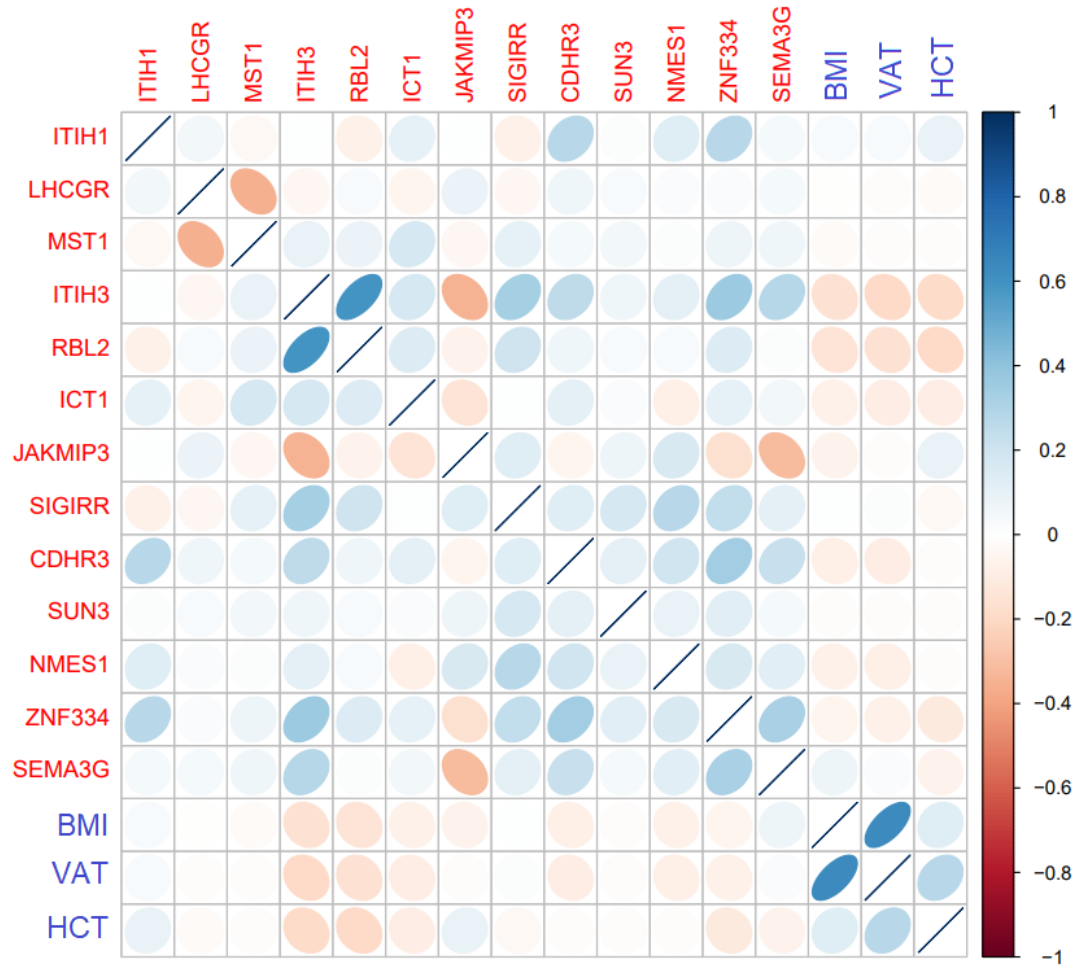
Supplementary Fig. S2. A Spearman rank correlation between all proteins as well as some quantitative traits including body mass index (BMI, kg/m2), visceral adipose tissue (VAT, measured *via* computed tomography) and hematocrit (HCT), that were associated with rs2251219.
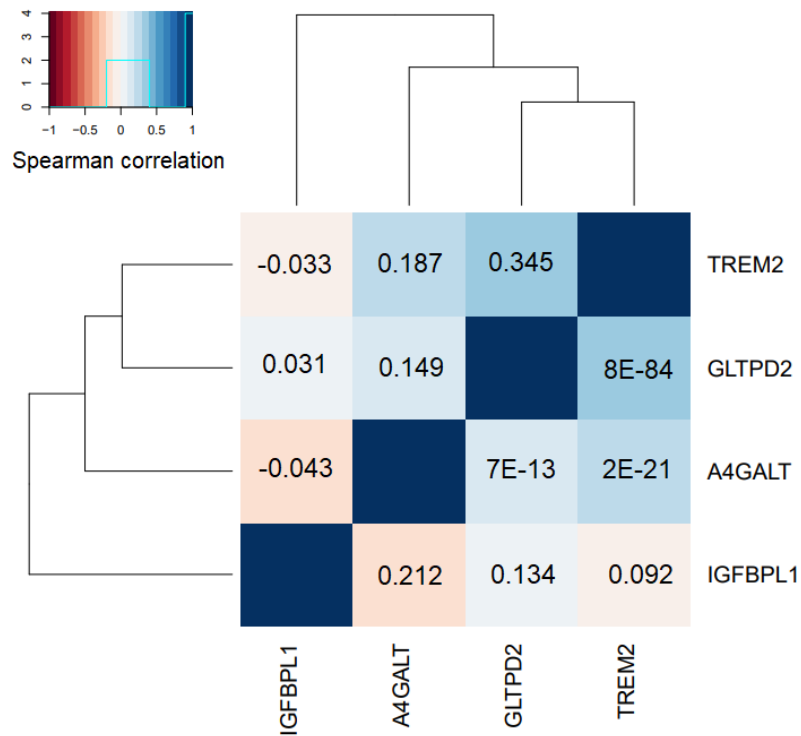
a
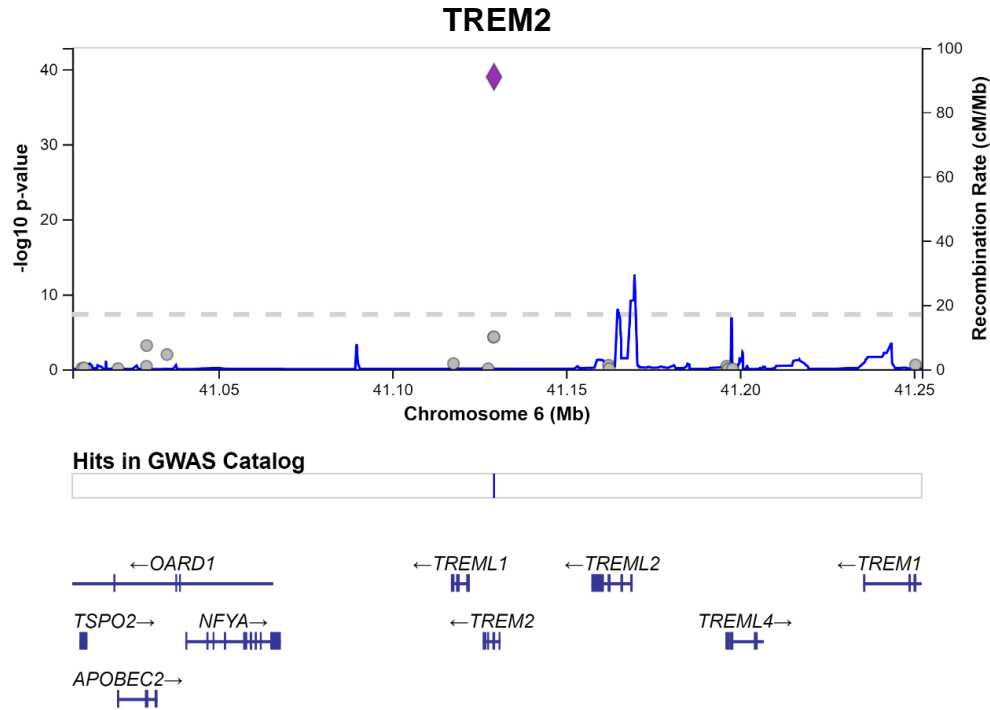
b
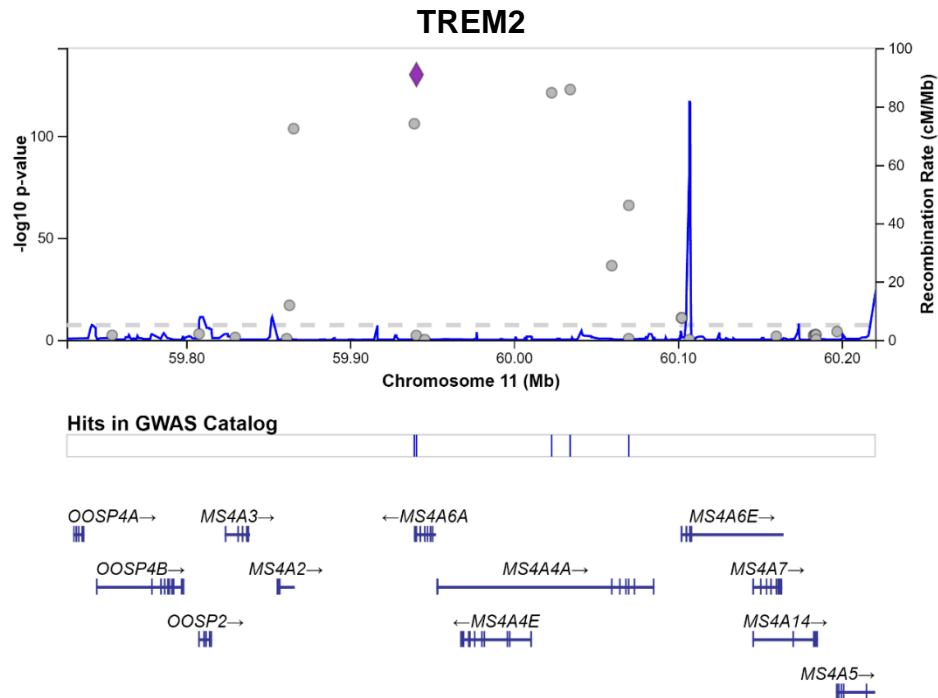
Supplementary Fig. S3. TREM2 regional plots (LocusZoom) based on exome array variants at chromosomes 6 and 11.
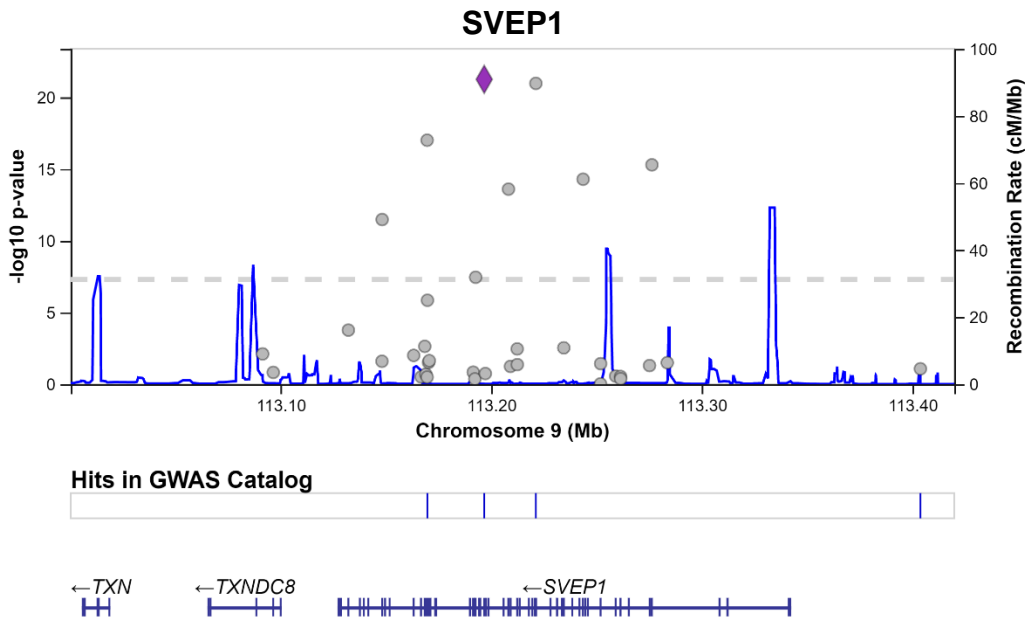
Supplementary Fig. S4. The graph shows the Spearman rank correlation between the four serum proteins affected by the two LOAD risk variants, rs75932628 and rs610932. The correlation matrix's upper triangle depicts the beta-values, while the lower triangle highlights the P-values.
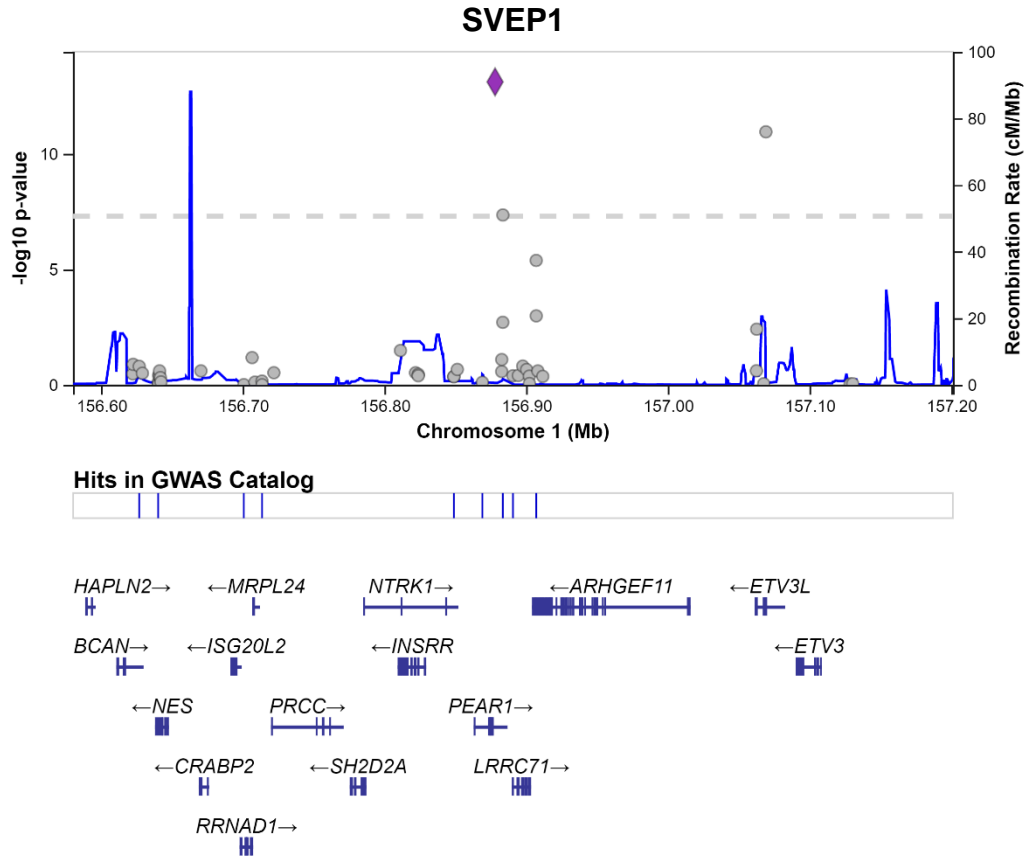
Supplementary Fig. S5. SVEP1 regional plots (LocusZoom) based on exome array variants at chromosomes 1 and 9.